Multiple Phase Equilibria in Polydisperse Polymer/Liquid Crystal Blends

C. C. Riccardi, J. Borrajo, and R. J. J. Williams*

Institute of Materials Science and Technology (INTEMA), University of Mar del Plata, 7600 Mar del Plata, Argentina, and National Research Council (CONICET), J. B. Justo 4302, 7600 Mar del Plata, Argentina

H. Masood Siddiqi, M. Dumon, and J. P. Pascault

Laboratoire des Matériaux Macromoléculaires (UMR CNRS No. 5627), Institut National des Sciences Appliquées de Lyon, 20 Av. Albert Einstein, F-69621 Villeurbanne Cedex, France

Received August 7, 1997; Revised Manuscript Received November 24, 1997

ABSTRACT: A thermodynamic analysis of phase equilibria in polydisperse polymer−liquid crystal blends is presented. Three different systems were analyzed: (a) a high molar mass polydisperse polystyrene (PS) blended with 4-cyano-4′-*n*-heptylbiphenyl (7CB), (b) a low molar mass polydisperse PS blended with 7CB, and (c) an epoxy-based thermosetting polymer blended with a mixture of small mesogenic molecules usually called E7. In the latter case the analysis was performed in both pregel and postgel stages. Macroscopic phase separation taking into account the fractionation of the polydisperse polymer among different phases, was simulated when cooling from an initially homogeneous state. Predicted isotropic−isotropic and isotropic−nematic transitions showed a good agreement with experimental results. The relative volume fraction and compositions of isotropic and nematic phases were predicted. A temperature range was found where three macroscopic phases, two isotropic and one nematic, coexisted at equilibrium. This was the result of a liquid−liquid (or gel−liquid) phase separation preceding the appearance of a nematic phase. Implications of this behavior on morphologies developed in polymer-dispersed liquid crystals (PDLC) are discussed.

Introduction

Many studies on the phase behavior of polymer/liquid crystal (LC) blends have been reported in recent years. Kronberg and Patterson[1] developed a simple theory for the nematic−isotropic equilibrium in the region of high LC concentrations. The theory was tested with a particular LC (*p*-ethoxybenzylidene−*p*-*n*-butylaniline, EBBA) with two series of polymeric solutes: polystyrene and poly(ethylene oxide).[2] Dubault et al.[3] presented the main types of phase diagrams obtained with flexible polymers in nematic solvents. Experimental data were compared with two theoretical descriptions. Ballauff et al.[4−6] used the extended Flory lattice theory to describe the phase behavior of polymer−LC blends, including liquid−liquid-phase separation in the isotropic phase. Kelkar and Manohar[7] and Shen and Kyu[8] extended the Flory−Huggins lattice theory of regular solutions to describe mixtures of nematic liquid crystals with non-nematic polymeric solutes. The nematic phase was described in terms of the Maier−Saupe approximation.[9,10] A similar approach was recently used to describe a diepoxide−diamine/LC blend, in pre- and postgel stages.[11] Cloud-point and shadow curves characteristic of isotropic−isotropic and nematic−isotropic equilibria, were generated in temperature vs composition coordinates in pre- and postgel stages. Experimental results for the isotropic−nematic transition could be reproduced by the numerical simulation using an interaction parameter inversely proportional to temperature and decreasing with conversion.

The existence of both liquid−liquid and liquid−nematic equilibria in polymer−LC blends has been theoretically predicted and experimentally demonstrated.[4−12] Usually these systems exhibit an upper-critical-solution-temperature behavior (UCST), meaning that at sufficiently high temperatures the blend remains homogeneous. When the blend cools from this temperature a thermally induced phase separation takes place. No previous thermodynamic analysis of polymer−LC blends has described the macroscopic phase separation, including polymer fractionation and multiple phase equilibria. This will be the aim of the present analysis. Comparison with experimental results will be shown and practical implications of the theoretical predictions will be discussed.

* To whom correspondence should be addressed at the University of Mar del Plata.

Thermodynamic Analysis

The blend consists of a liquid crystal (LC, component 1) and a polymer with a known distribution of molar masses (component 2). To describe the free energy of the mixture using a Flory−Huggins lattice model, the unit cell is assigned a molar volume V_r. The number of moles of cells occupied by one mol of LC of molar volume V_{LC}, is

$$r_1 = V_{LC}/V_r \tag{1}$$

The corresponding value for a polymeric species i with molar volume V_i, is

$$r_i = V_i/V_r \tag{2}$$

For a mixture of n_1 moles of LC and a known distribution of n_i moles of polymer, the free energy of mixing in an isotropic phase may be expressed by the

S0024-9297(97)01206-0 CCC: $15.00 © 1998 American Chemical Society
Published on Web 01/31/1998

Flory−Huggins equation, as

$$\Delta G^{I}/RT = n_1^{I} \ln \phi_1^{I} + \sum n_i^{I} \ln \phi_i^{I} + r_1 n_1^{I} \chi \phi_2^{I} \quad (3)$$

where $\phi_1 = n_1 r_1/(n_1 r_1 + \sum n_i r_i)$, is the volume fraction of LC, $\phi_2 = \sum \phi_i = 1 - \phi_1$, is the volume fraction of polymer and χ is the interaction parameter assumed to be a function of temperature.

Chemical potentials in the isotropic phase may be obtained from the partial derivatives of eq 3,

$$\Delta\mu_1^{I}/RT = 1 + \ln \phi_1^{I} - r_1[(\phi_1^{I}/r_1) + (\phi_2^{I}/r_2^{I})] + r_1\chi(\phi_2^{I})^2 \quad (4)$$

$$\Delta\mu_i^{I}/RT = 1 + \ln \phi_i^{I} - r_i[(\phi_1^{I}/r_1) + (\phi_2^{I}/r_2^{I})] + r_i\chi(\phi_1^{I})^2 \quad (5)$$

where

$$r_2^{I} = \phi_2^{I}/\sum(\phi_i^{I}/r_i) \quad (6)$$

In a nematic phase the free energy of mixing may be expressed combining Flory−Huggins and Maier−Saupe theories[7,8]

$$\Delta G^{N}/RT = n_1^{N} \ln \phi_1^{N} + \sum n_i^{N} \ln \phi_i^{N} + r_1 n_1^{N} \chi \phi_2^{N} + (\nu/2)\phi_1^{N} n_1^{N} s^2 - n_1^{N} \ln Z \quad (7)$$

where ν is the Maier−Saupe quadrupole interaction parameter, given by:

$$\nu = 4.54 T_{I-N}/T \quad (8)$$

and T_{I-N} is the isotropic−nematic transition temperature of the neat liquid crystal.

Z is the orientational partition function for the nematic component of the mixture

$$Z = \int_0^1 \exp[(m/2)(3\cos^2\theta - 1)]\, d(\cos\theta) \quad (9)$$

where θ is the angle between a reference axis and the director of a liquid crystal molecule, and m is a mean field parameter characterizing the strength of the potential field

$$m = \phi_1^{N} \nu s \quad (10)$$

The orientational order parameters is defined as

$$s = (1/Z)\int_0^1 (1/2)\,(3\cos^2\theta - 1)\exp[(m/2)(3\cos^2\theta - 1)]\, d(\cos\theta) \quad (11)$$

By expanding the exponential function in series, Z and s may be calculated by

$$Z = \exp(-m/2)\sum_{n=0}^{\infty}(1.5m)^n/[n!(2n+1)] \quad (12)$$

$$s = (\sum_{n=0}^{\infty} 1.5\,(1.5m)^n/[n!(2n+3)])/(\sum_{n=0}^{\infty}(1.5m)^n/[n!(2n+1)]) - 0.5 \quad (13)$$

Both functions are rapidly convergent being useful for computational calculations.

Chemical potentials in the nematic phase may be obtained from the partial derivatives of eq 7

$$\Delta\mu_1^{N}/RT = 1 + \ln \phi_1^{N} - r_1[(\phi_1^{N}/r_1) + (\phi_2^{N}/r_2^{N})] + r_1\chi(\phi_2^{N})^2 + (\nu/2)(s\phi_1^{N})^2 - \ln Z \quad (14)$$

$$\Delta\mu_i^{N}/RT = 1 + \ln \phi_i^{N} - r_i[(\phi_1^{N}/r_1) + (\phi_2^{N}/r_2^{N})] + r_i\chi(\phi_1^{N})^2 + (r_i/r_1)(\nu/2)(s\phi_1^{N})^2 \quad (15)$$

where

$$r_2^{N} = \phi_2^{N}/\sum(\phi_i^{N}/r_i) \quad (16)$$

Different general situations will be now analyzed.

Equilibrium between Two Isotropic Liquid Phases. Let us call $R = V^{\beta}/V_T$, the volume fraction of the isotropic phase richer in LC (β-phase), and $1 - R = V^{\alpha}/V_T$, the volume fraction of isotropic phase richer in polymer. The following mass balances may be written

$$\phi_1^{0} = (1 - R)\phi_1^{\alpha} + R\phi_1^{\beta} \quad (17)$$

$$\phi_i^{0} = (1 - R)\phi_i^{\alpha} + R\phi_i^{\beta} \quad (18)$$

where ϕ_1^0 and ϕ_i^0 are, respectively, the volume fractions of LC and polymeric species in the initial blend.

At equilibrium

$$\Delta\mu_1^{I}(\alpha) = \Delta\mu_1^{I}(\beta) \quad (19)$$

$$\Delta\mu_i^{I}(\alpha) = \Delta\mu_i^{I}(\beta) \quad (20)$$

Replacing eqs 4 and 5 and rearranging, we obtain the following equations for the separation factors:

$$\sigma_1 = (1/r_1)\ln(\phi_1^{\beta}/\phi_1^{\alpha}) = [(\phi_1^{\beta}/r_1 + \phi_2^{\beta}/r_2^{\beta}) - (\phi_1^{\alpha}/r_1 + \phi_2^{\alpha}/r_2^{\alpha})] + \chi[(\phi_2^{\alpha})^2 - (\phi_2^{\beta})^2] \quad (21)$$

$$\sigma_2 = (1/r_i)\ln(\phi_i^{\beta}/\phi_i^{\alpha}) = [(\phi_1^{\beta}/r_1 + \phi_2^{\beta}/r_2^{\beta}) - (\phi_1^{\alpha}/r_1 + \phi_2^{\alpha}/r_2^{\alpha})] + \chi[(\phi_1^{\alpha})^2 - (\phi_1^{\beta})^2] \quad (22)$$

Replacing the definitions of σ_1 and σ_2 in eqs 17 and 18, leads to the following expressions:

$$\phi_1^{\alpha} = \phi_1^{0}/(1 + R[\exp(\sigma_1 r_1) - 1]) \quad (23)$$

$$\phi_i^{\alpha} = \phi_i^{0}/(1 + R[\exp(\sigma_2 r_i) - 1]) \quad (24)$$

$$\phi_2^{\alpha} = \sum\phi_i^{\alpha} \quad (25)$$

$$\phi_1^{\beta} = \phi_1^{0}\exp(\sigma_1 r_1)/(1 + R[\exp(\sigma_1 r_1) - 1]) \quad (26)$$

$$\phi_i^{\beta} = \phi_i^{0}\exp(\sigma_2 r_i)/(1 + R[\exp(\sigma_2 r_i) - 1]) \quad (27)$$

$$\phi_2^{\beta} = \sum\phi_i^{\beta} \quad (28)$$

The set of eqs 21−28 could be solved to calculate the composition and volume fraction of the two macroscopic liquid phases at equilibrium, as a function of temperature. Input parameters were $\chi(T)$ and the initial composition of the blend including the distribution of polymeric species.

Equilibrium between a Nematic Phase and an Isotropic Liquid Phase. Let us call $S = V^N/V_T$, the volume fraction of the nematic phase, and $1 - S$, the volume fraction of the isotropic phase. The following mass balances must hold:

$$\phi_1^0 = (1 - S)\phi_1^I + S\phi_1^N \quad (29)$$

$$\phi_i^0 = (1 - S)\phi_i^I + S\phi_i^N \quad (30)$$

At equilibrium

$$\Delta\mu_1^I = \Delta\mu_1^N \quad (31)$$

$$\Delta\mu_i^I = \Delta\mu_i^N \quad (32)$$

Replacing eqs 4, 5, 14, and 15 and rearranging leads to the following expressions for the separation factors:

$$\sigma_3 = (1/r_1)\ln(\phi_1^N/\phi_1^I) = [(\phi_1^N/r_1 + \phi_2^N/r_2^N) - (\phi_1^I/r_1 + \phi_2^I/r_2^I)] + \chi[(\phi_2^I)^2 - (\phi_2^N)^2] - (\nu/2r_1)(s\phi_1^N)^2 + (1/r_1)\ln Z \quad (33)$$

$$\sigma_4 = (1/r_i)\ln(\phi_i^N/\phi_i^I) = [(\phi_1^N/r_1 + \phi_2^N/r_2^N) - (\phi_1^I/r_1 + \phi_2^I/r_2^I)] + \chi[(\phi_1^I)^2 - (\phi_1^N)^2] - (\nu/2r_1)(s\phi_1^N)^2 \quad (34)$$

Replacing the definitions of σ_3 and σ_4 in eqs 29 and 30, leads to

$$\phi_1^I = \phi_1^0/(1 + S[\exp(\sigma_3 r_1) - 1]) \quad (35)$$

$$\phi_i^I = \phi_i^0/(1 + S[\exp(\sigma_4 r_i) - 1]) \quad (36)$$

$$\phi_2^I = \sum\phi_i^I \quad (37)$$

$$\phi_1^N = \phi_1^0 \exp(\sigma_3 r_1)/(1 + S[\exp(\sigma_3 r_1) - 1]) \quad (38)$$

$$\phi_i^N = \phi_i^0 \exp(\sigma_4 r_i)/(1 + S[\exp(\sigma_4 r_i) - 1]) \quad (39)$$

$$\phi_2^N = \sum\phi_i^N \quad (40)$$

The set of eqs 33−40 could be solved to calculate the composition and volume fractions of isotropic and nematic phases at equilibrium, as a function of temperature. Input parameters were $\chi(T)$, the initial composition of the blend including the distribution of polymeric species, and T_{I-N} of the LC.

Equilibria among Two Isotropic Liquid Phases and a Nematic Phase. The following mass balances may be written

$$\phi_1^0 = (1 - R - S)\phi_1^\alpha + R\phi_1^\beta + S\phi_1^N \quad (41)$$

$$\phi_i^0 = (1 - R - S)\phi_i^\alpha + R\phi_i^\beta + S\phi_i^N \quad (42)$$

At equilibrium, eqs 19, 20, 31, and 32 must hold simultaneously. The separation factors σ_1 to σ_4 keep their definitions given by eqs 21, 22, 33, and 34 (with I = α). Replacing these definitions in eqs 41 and 42, leads to

$$\phi_1^\alpha = \phi_1^0/(1 + R[\exp(\sigma_1 r_1) - 1] + S[\exp(\sigma_3 r_1) - 1]) \quad (43)$$

$$\phi_i^\alpha = \phi_i^0/(1 + R[\exp(\sigma_2 r_i) - 1] + S[\exp(\sigma_4 r_i) - 1]) \quad (44)$$

$$\phi_2^\alpha = \sum\phi_i^\alpha \quad (45)$$

$$\phi_1^\beta = \phi_1^0 \exp(\sigma_1 r_1)/(1 + R[\exp(\sigma_1 r_1) - 1] + S[\exp(\sigma_3 r_1) - 1]) \quad (46)$$

$$\phi_i^\beta = \phi_i^0 \exp(\sigma_2 r_i)/(1 + R[\exp(\sigma_2 r_i) - 1] + S[\exp(\sigma_4 r_i) - 1]) \quad (47)$$

$$\phi_2^\beta = \sum\phi_i^\beta \quad (48)$$

$$\phi_1^N = \phi_1^0 \exp(\sigma_3 r_1)/(1 + R[\exp(\sigma_1 r_1) - 1] + S[\exp(\sigma_3 r_1) - 1]) \quad (49)$$

$$\phi_i^N = \phi_i^0 \exp(\sigma_4 r_i)/(1 + R[\exp(\sigma_2 r_i) - 1] + S[\exp(\sigma_4 r_i) - 1]) \quad (50)$$

$$\phi_2^N = \sum\phi_i^N \quad (51)$$

The sets of eqs 21, 22, 33, and 34 (with I = α) and eqs 43−51 could be solved to calculate the compositions and volume fractions of the three phases at equilibrium, as a function of temperature. Input parameters were $\chi(T)$, the initial composition of the blend including the distribution of polymeric species, and T_{I-N} of the LC.

Results and Discussion

PS (M_n = 152 000)/7CB Blend. The phase diagram of a high molar mass polydisperse polystyrene (PS) blended with a LC, 4-cyano-4′-*n*-heptylbiphenyl (7CB), was reported by Ahn et al.[12] It was constructed from DSC (differential scanning calorimetry) and optical microscopic observations both in phase contrast and cross-polarized modes. Figure 1 shows reported experimental values of L−L phase separation, appearance of a nematic phase, and onset of vitrification. Experimental points located below the L−L and L−N curves simply indicate the temperature at which the particular transition, i.e., isotropic−nematic or vitrification, was observed for a given initial composition. But the actual phase composition is not the initial one due to the previous L−L phase separation.

The input data necessary for the thermodynamic analysis will be now considered. The molar mass distribution of PS was obtained using the reported number and mass averages in the Schulz-Zimm equation[13]

$$w(i) = [g^{h+1}/\Gamma(h + 1)]i^h \exp(-gi) \quad (52)$$

where $w(i)$ is the mass fraction of the i-mer, $h = [(x_w/x_n) - 1]^{-1}$, $g = h/x_n$, and Γ is the gamma function. For the particular PS used by Ahn et al.,[12] $x_w/x_n = 1.9079$,

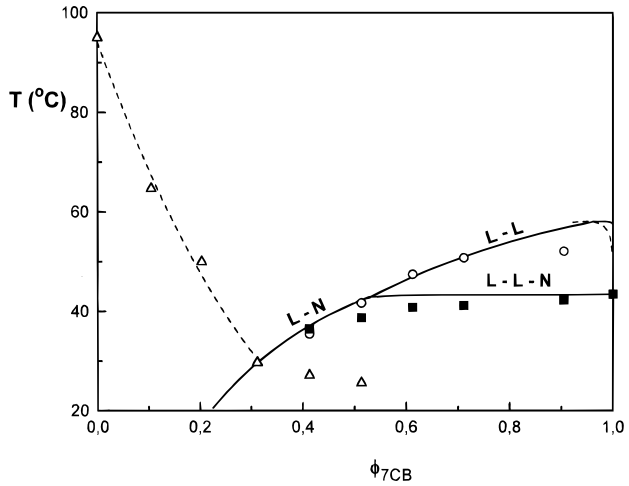

Figure 1. Phase diagram of PS (M_n = 152 000)−7CB blend showing experimental values of L−L phase separation (○), appearance of a nematic phase (■) and vitrification (△), reported by Ahn et al.,[12] and predicted L−L, L−N, and L−L-N equilibria using χ vs T given by eq 54 (the shadow curve for the L−L equilibrium is represented by the dashed line at high LC concentrations).

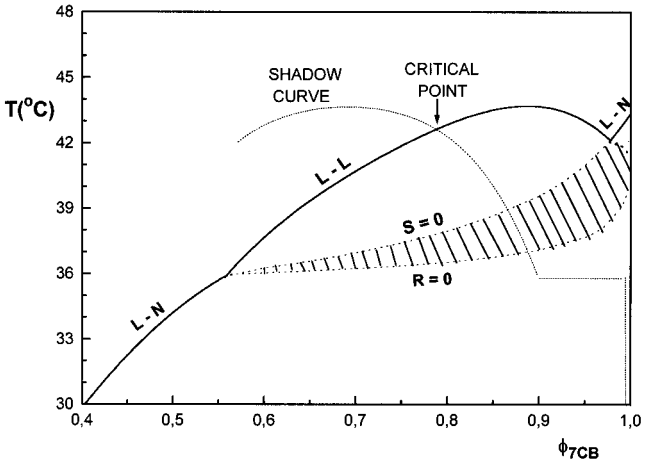

Figure 2. Phase diagram of the PS (M_n = 3000)−7CB blend, indicating the predicted CPC for L−L and L−N equilibria, the shadow curves (dotted lines) and the critical point. The curve for S = 0 corresponds to the first appearance of a nematic phase when cooling; the curve for R = 0 indicates the disappearance of the isotropic β-phase when cooling. The shaded area is the region where three phases (two isotropic and one nematic) coexist at equilibrium.

h = 1.1014, and $g = 7.536 \times 10^{-4}$. The initial volume fraction of i-mers is given by:

$$\phi_i^0 = w(i)\phi_2^0 \tag{53}$$

The numerical solution was performed using 15 000 chains with the Schulz−Zimm distribution.

The molar volume of a constitutional repeating unit of PS is V_r = 98.113 cm^3/mol, taken as the reference volume. The corresponding molar volume of 7CB is V_{7CB} = 274.4 cm^3/mol. Then, $r_i = i$ and r_1 = 2.797. The isotropic−nematic transition temperature of 7CB is T_{I-N} = 316.5 K.

Equations for L−L equilibrium were solved to fit the interaction parameter from experimental values of cloud-point temperatures. The following relationship was obtained:

$$\chi = -1.445 + 541.3/T\ (\mathrm{K}) \tag{54}$$

Figure 1 shows the predicted phase diagram for the PS/7CB blend, including the boundaries for L−L, L−N, and the simultaneous L−L−N equilibria. The shadow curve, indicating the compositions of the phase segregated at the cloud point, is depicted with the dashed line at high LC concentrations (the intersection of the CPC and the shadow curve is the critical point).

Due to its high average molar mass, the PS is practically excluded from the LC-rich phase (β-phase). For example, for $\phi_1^0 = 0.8$, the cloud-point temperature is T = 54.1 °C and the composition of the β-phase, read at the shadow curve, is $\phi_1^\beta = 0.9956$, i.e., practically pure LC. When the temperature is decreased, the composition of the α-phase follows a trajectory practically superimposed on the CPC while the β-phase still increases its LC concentration. At T = 43.38 °C, a simultaneous L−L−N equilibria is predicted. At this temperature, $\phi_1^\alpha = 0.5380$, $\phi_1^\beta = 0.99996$, and $\phi_1^N \rightarrow 1$ (R = 0.567 and S = 0). Continuing the cooling leads to the disappearance of the β-phase and the establishment of a L (α-phase)−N equilibrium.

Therefore, due to the high molar mass of PS, both the β-phase and the nematic phase consist of practically pure LC (except for a small region located close to the critical point). For practical purposes the composition of the α-phase may be read at the L−L or L−N curves and the compositions of the β-phase and the nematic phase may be considered as consisting of pure LC. The lever rule, giving the relative amount of phases at equilibrium, is applicable.

To simulate the fractionation effect, we will analyze the case of a PS with M_n = 3000, keeping the same polydispersity as for the high molar mass PS.

PS (M_n = 3000)/7CB Blend. The molar mass distribution of the PS is obtained from eq 52 with x_w/x_n = 1.9079, h = 1.1014, and $g = 3.818 \times 10^{-2}$. In this case the numerical solution was obtained using 415 chains with the Schulz−Zimm distribution. The interaction parameter with 7CB is given by eq 54.

Figure 2 shows the calculated phase diagram in temperature vs composition coordinates. Several differences with the corresponding diagram for the high molar mass PS are evident. First, the L−N equilibrium reappears at high LC concentrations. Therefore, when cooling blends with compositions $\phi_{7CB} < 0.558$ or $\phi_{7CB} > 0.976$, a nematic phase will be segregated from the initial solution. In the intermediate range a L−L phase separation will occur. The critical point is located at $\phi_{7CB} = 0.79$. For $0.558 \le \phi_{7CB} < 0.79$, the liquid phase demixed at the cloud point will be richer in the LC than the starting solution (composition read at the shadow curve). The opposite situation is observed at the right of the critical point.

The curve for S = 0 indicates the appearance of a nematic phase simultaneously in both liquid phases (this is the consequence of establishing equality in chemical potentials in the three phases at equilibrium). The curve for R = 0 indicates the complete disappearance of the liquid phase with the higher LC concentration. Below the curve R = 0, the system consists of a L and a N phase at equilibrium. In the shaded region that lies between the curves S = 0, R = 0, and their intersection with the curve for R = 1 at high ϕ_{7CB} values, three macroscopic phases (two isotropic and one nematic) coexist at equilibrium. It is observed that the temperature at which a nematic phase first appears

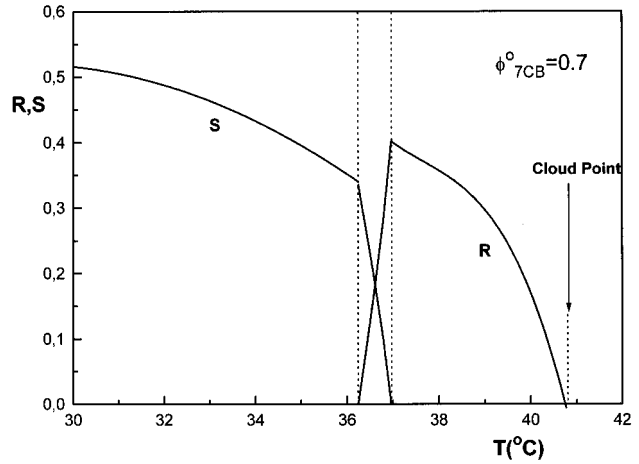

Figure 3. Evolution of volume fractions of β-phase (R) and nematic phase (S) when cooling a PS (M_n = 3000)−7CB blend with $\phi_{7CB}^{\circ} = 0.7$.

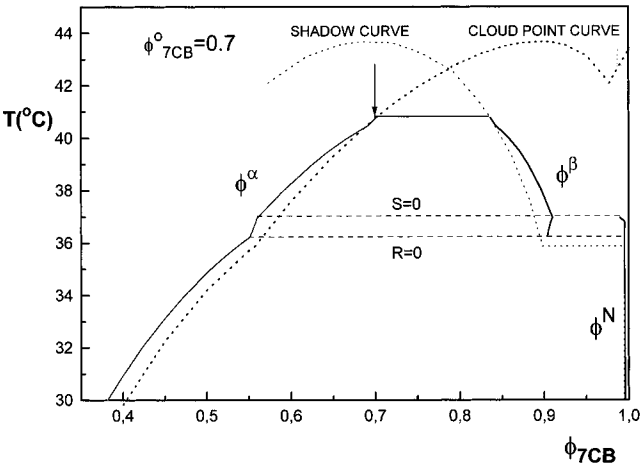

Figure 4. Evolution of the equilibrium composition of phases generated when cooling a PS (M_n = 3000)−7CB blend with $\phi_{7CB}^{\circ} = 0.7$. Full lines represent coexistence curves; dashed lines represent cloud-point and shadow curves.

when cooling increases continuously with ϕ_{7CB}. Thus, T_{I-N} is about 36 °C for $\phi_{7CB} = 0.558$, 39 °C for $\phi_{7CB} = 0.87$ and 43.5 °C for $\phi_{7CB} = 1$.

Figure 3 shows the evolution of volume fractions of liquid phase rich in LC (R) and of nematic phase (S), when cooling a blend containing a LC volume fraction, $\phi_{7CB}^{\circ} = 0.7$. L−L phase separation begins at the cloud point located at T = 40.8 °C. The volume fraction of LC-rich phase (β-phase) increases up to $R = 0.38$ at T close to 37 °C. At this temperature a nematic phase appears in the system. Decreasing T by about 0.75 °C leads to the complete disappearance of the β-phase ($R = 0$) and a corresponding increase in the volume fraction of the nematic phase up to $S = 0.33$. Continuing the cooling increases the volume fraction of nematic phase. The evolution of the composition of these phases is shown in Figure 4. Compositions of α- and β-phases diverge from the CPC and the shadow curve, as expected (for the high molar mass PS the departure of the coexistence curve from cloud-point and shadow curves was not significant except for a small region located close to the critical point). In the range where three phases coexist, the β-phase is transformed into α and nematic phases. The latter contains a very small amount of the low molar mass fraction of the PS distribution.

The numerical solution gives the equilibrium state predicted by the thermodynamic model. In practice, the ratio of the phase separation kinetics with the cooling rate will determine the actual approach to the equilibrium state. But, even with this restriction, some general features of the evolution of morphologies may be predicted. For example, for the blend with $\phi_{7CB}^{\circ} = 0.7$, droplets of the β-phase will be generated in the 40.8−37 °C range, attaining a maximum volume fraction, $R = 0.38$. At T close to 37 °C a nematic phase will begin to be segregated from both isotropic phases. Because of the different concentrations and viscosities of both phases, segregated nematic domains may exhibit different morphologies. This situation may be avoided by decreasing the initial LC concentration to $\phi_{7CB}^{\circ} < 0.558$. Cooling these compositions will lead to a single isotropic−nematic phase separation process.

Thermosetting Epoxy−E7 Blend. To compare thermodynamic predictions with experimental results, macroscopic phase separation in a blend of a thermosetting epoxy with a LC will be analyzed. A thermodynamic analysis of the reaction-induced phase separation in this blend has been recently presented.[11] The analysis was restricted to the prediction of cloud-point curves for isotropic−isotropic (I−I) and isotropic−nematic (I−N) equilibria, covering the whole conversion range in both pregel and postgel stages. It will be now extended to account for the macroscopic phase separation produced by cooling or advancing the conversion beyond the cloud point.

The epoxy (DER 332, Dow) was based on diglycidyl ether of bisphenol A (DGEBA), a difunctional monomer with a number-average molar mass, M_n = 348.5 g/mol, and a molar volume equal to V_{DGEBA} = 298 cm^3/mol. The hardener was a polypropyleneoxide diamine (Jeffamine D-400, Texaco), a tetrafunctional monomer with a number-average molar mass, M_n = 398.8 g/mol, and a molar volume equal to V_{DA} = 364 cm^3/mol. Both monomers were used in stoichiometric proportions. The LC was a mixture of small mesogenic molecules usually called E7 (BL001, E-Merck), with an average molar volume of V_{LC} = 268 cm^3/mol. E7 exhibits an isotropic−nematic transition at T_{I-N} = 59.5 °C.

An epoxy/diamine−E7 blend with an initial composition $\phi_{LC}^{\circ} = 0.531$, was partially reacted at 100 °C to conversions comprised in the 0.3−0.8 range (determined by DSC) and then cooled at 1 K/min to determine the isotropic−nematic transition temperature by polarized optical microscopy (POM). Alternatively, the reaction was carried out at constant temperature (20 or 30 °C), and the conversion of the isotropic−nematic transition was determined (POM combined with DSC). To provide a comparison of these experimental results with thermodynamic predictions is the aim of this section.

The thermodynamic analysis must be adapted for the present case. It is convenient to analyze the pregel stage separately from the postgel stage. In the pregel stage, the distribution of oligomeric epoxy−amine species, E_{ij}, containing i diamine (DA) and j diepoxide (DGEBA) molecules, is given by the Stockmayer distribution function[14,15]

$$E_{ij} = [\mathrm{DA}]_0\,[4(3i)!p^{i+j-1}(1-p)^{2i+2}]/[i!(3i-j+1)!(j-i+1)!] \quad (55)$$

where p is conversion and $[DA]_0$ is the initial molar concentration of DA in the blend. Equation 55 assumes

that the polycondensation is ideal, i.e., equal reactivity of functional groups, no substitution effects, and no intramolecular cycles. The particular epoxy/amine system devoid of LC showed an ideal behavior as revealed by the gel conversion value and the equal reactivity of secondary and primary amine hydrogens.[16] In the presence of LC, secondary amine hydrogens were less reactive than primary amine ones. This factor together with the possible presence of intramolecular cyclization produced a slight increase of the experimental gel conversion from the ideal value of 0.577 to 0.62.[16] However, in the present simulation it will be assumed that eq 55 provides a reasonable estimation of the distribution of oligomeric species in the pregel stage.

The volume fraction of an E_{ij} species is given by

$$\phi_{ij} = E_{ij}V_{ij} = E_{ij}\,[iV_{DA} + jV_{DGEBA}] \tag{56}$$

where V_{ij} is the molar volume of E_{ij}.

The volume fraction of thermosetting polymer in the blend is obtained from

$$\phi_2 = \sum\sum\phi_{ij} \tag{57}$$

The reference volume is taken as the molar volume of LC, V_{LC}. Then, $r_1 = 1$ and $r_{ij} = V_{ij}/V_{LC}$. General equations may be applied to this particular system by replacing ϕ_i by ϕ_{ij} and r_i by r_{ij}.

The interaction parameter was fitted by the following relationship:[11]

$$\chi = -0.115 + 404.2/T\,(\mathrm{K}) - 0.267p \tag{58}$$

Equation 58 must be regarded as a phenomenological expression characterizing the partially reacted material. It accounts for the fact that the disappearance of epoxy and amine groups through polycondensation makes the resulting chemical structure more compatible with the LC, a fact reflected by the decrease of χ with conversion. Similar observations were made for rubber-modified cyanate esters[17] and poly(ether imide)-modified epoxies.[18]

To solve the set of equations in the pregel stage it was necessary to truncate the distribution of E_{ij} species at selected values of i_{max} and j_{max}. These values were defined such that the mass-average molar mass of the generated distribution agreed with the theoretical prediction[14] within an error of 0.5%. The number of species to be considered increased significantly for conversions close to $p_{gel} = 0.577$. So, numerical simulations in the pregel stage were performed up to conversions equal to $p = 0.5$.

The analysis in the postgel stage requires the knowledge of the evolution of the volume fractions of sol, ϕ_s, and gel, ϕ_g, as a function of conversion and the distribution of oligomeric species in the sol E_{ij}(sol).

The volume fraction of thermosetting polymer in the mixture with LC is given by

$$\phi_2 = \phi_s + \phi_g \tag{59}$$

where

$$\phi_s = \sum\sum\phi_{ij} = \sum\sum E_{ij}(\mathrm{sol})[iV_{DA} + jV_{DGEBA}] \tag{60}$$

$$\phi_g = \phi_s\,(1 - w_s)/w_s \tag{61}$$

The mass fraction of sol, w_s, is obtained from[19,20]

$$w_s = w_{DA}x^4 + w_{DGEBA}(px^3 + 1 - p)^2 \tag{62}$$

where

$$x = [(1/p^2) - 0.75]^{1/2} - 0.5 \tag{63}$$

is the probability of seeing a finite chain when looking out from a random chosen amine hydrogen, and w_{DA} and w_{DGEBA} are the mass fractions of both monomers (defined such that their sum is equal to 1).

E_{ij}(sol) may be calculated from the Stockmayer distribution function[13]

$$E_{ij}(\mathrm{sol}) = [\mathrm{DA}]_0x^4[4(1 - p_{As})(1 - p_{Bs})/p_{Bs}][(3i)!j!(\gamma^i/i!) \times (\delta^j/j!)]/[(3i - j + 1)!(j - i + 1)!] \tag{64}$$

where $[DA]_0$ is the initial molar concentration of DA in the blend and

$$\gamma = p_{Bs}\,(1 - p_{As})^3/(1 - p_{Bs}) \tag{65}$$

$$\delta = p_{As}\,(1 - p_{Bs})/(1 - p_{As}) \tag{66}$$

$$p_{As} = (p/x)\,(px^3 + 1 - p) \tag{67}$$

$$p_{Bs} = px^3/(px^3 + 1 - p) \tag{68}$$

Three different phases may be present in the postgel stage of the thermosetting polymer−E7 blend, i.e., one isotropic phase containing gel, sol, and LC, another isotropic phase composed of sol and LC, and a nematic phase constituted of sol and LC. Expressions for the chemical potentials of the isotropic phase devoid of gel (liquid phase) and the nematic phase are those derived in the general thermodynamic section. The corresponding equations for the isotropic phase containing gel (gel phase), are[11]

$$\Delta\mu_1^G/RT = 1 + \ln\phi_1^G - r_1[(\phi_1^G/r_1) + (\phi_s^G/r_s^G)] + r_1\chi(\phi_2^G)^2 + r_1\nu_eV_{LC}\,(\phi_g^G)^{1/3}/3 \tag{69}$$

$$\Delta\mu_{ij}^G/RT = 1 + \ln\phi_{ij}^G - r_{ij}[(\phi_1^G/r_1) + (\phi_s^G/r_s^G)] + r_{ij}\chi(\phi_1^G)^2 + r_{ij}\nu_eV_{LC}\,(\phi_g^G)^{1/3}/3 \tag{70}$$

where ν_e is the concentration of elastic chains per unit volume of gel, given by[11]

$$\nu_e = [(1 - x)^4 + 2x\,(1 - x)^3]/[w_g(V_{DA} + 2V_{DGEBA})] \tag{71}$$

and

$$r_s^G = \phi_s^G/\sum\sum(\phi_{ij}^G/r_{ij}) \tag{72}$$

The elastic contribution to the free energy is based on the phantom network model with elastic chains counted as the DA units attached to trifunctional cross-linking points.[11]

The numerical solution in the postgel stage was obtained for $p \geq 0.70$, where the truncation error of the distribution E_{ij}(sol) was such that the calculated mass-average molar mass of the sol agreed with the theoretical value[20] within an error of 0.5%. Therefore, the

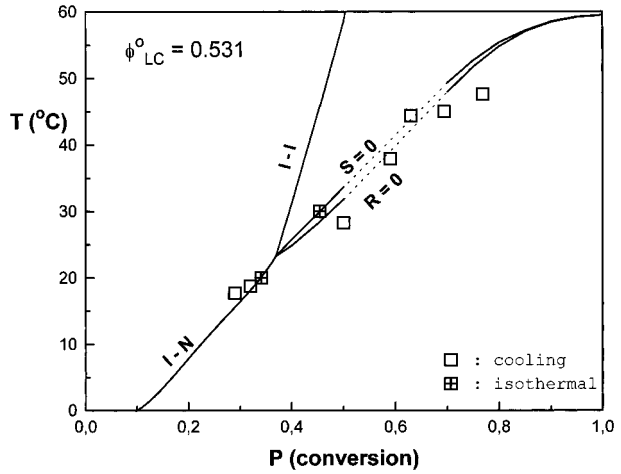

Figure 5. Phase transformation diagram of the thermosetting epoxy−E7 blend in temperature vs conversion coordinates, for $\phi_{LC}^{\circ} = 0.531$. Experimental points for the isotropic−nematic transition temperature were obtained by advancing the reaction at 100 °C and cooling (□) or under isothermal reaction conditions (+).

solution of thermodynamic equations for the thermosetting epoxy−E7 blend was obtained in the conversion range $0 \le p \le 0.5$ (pregel stage) and $0.7 \le p \le 1$ (postgel stage).

The predicted phase transformation diagram, in temperature vs conversion coordinates, is shown in Figure 5 for a particular blend with an initial liquid crystal concentration equal to $\phi_{LC}^{\circ} = 0.531$ (50 wt %). Experimental points for the isotropic−nematic transition were obtained either by advancing the reaction at 100 °C and cooling at 1 K/min or by reacting at a constant temperature (the isotropic−isotropic transition could not be detected possibly due to the small difference in the refractive index of both phases). The thermodynamic model exhibits a satisfactory predictive behavior, even considering the arbitrary interpolation in the 0.5−0.7 conversion range. For $p < 0.37$, the I−N transition takes place directly from the homogeneous blend. For $p \ge 0.37$ an I−I phase separation precedes the I−N transition. The curve for $S = 0$ indicates the simultaneous appearance of a nematic phase in both isotropic phases previously separated (a L−L equilibrium in the pregel stage and a gel−L equilibrium in the postgel stage). In the region comprising the area between the $R = 0$ and $S = 0$ curves, three phases coexist at equilibrium. The curve for $R = 0$ marks the disappearance of the L phase rich in LC (β-phase). Below this curve there is an equilibrium between two phases, i.e., the α-phase (liquid or gel) and a nematic phase.

Figure 6 shows the predicted evolution of volume fractions of β-phase (R) and nematic phase (S), when the epoxy−E7 blend, previously reacted to a conversion $p = 0.45$, was cooled. At $T = 44.7$ °C the β-phase appears in the system. Its volume fraction increases to $R = 0.254$ at $T = 29.7$ °C, the temperature at which the nematic phase makes its appearance. Decreasing T by about 1.6 °C makes the β-phase completely disappear and causes the nematic phase to increase its volume fraction to $S = 0.146$. Further cooling produces a continuous increase in the volume fraction of nematic phase. Figure 7 shows the evolution of the equilibrium compositions of different phases during the cooling process. Below the cloud-point temperature the trajectories of α- and β-phase compositions diverge from the

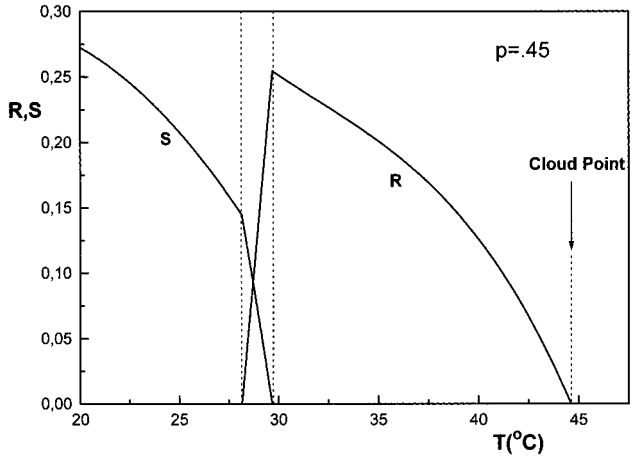

Figure 6. Evolution of volume fractions of β-phase (R) and nematic phase (S) when cooling the epoxy−E7 blend ($\phi_{LC}^{\circ} = 0.531$), previously reacted to a conversion $p = 0.45$.

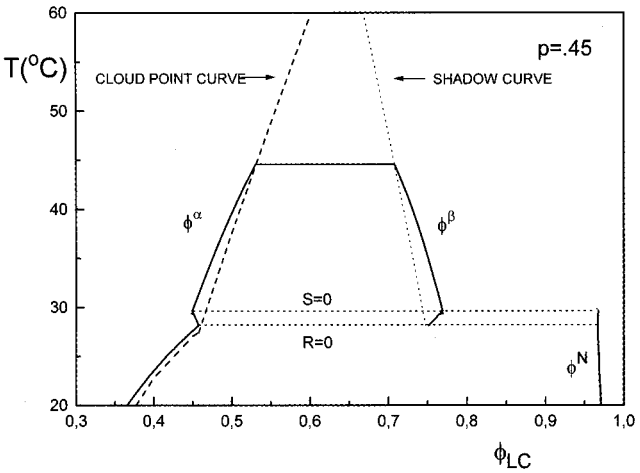

Figure 7. Evolution of the equilibrium composition of phases generated when cooling the epoxy−E7 blend ($\phi_{LC}^{\circ} = 0.531$), previously reacted to a conversion $p = 0.45$. Full lines represent coexistence curves; dashed lines represent cloud-point and shadow curves.

CPC and shadow curve. In the temperature range 28.1−29.7 °C, three macroscopic phases (α, β and N) coexist at equilibrium. The β-phase is partially transformed into a nematic phase exhibiting a high LC concentration. The partial dissolution of the β-phase causes the α-phase to increase slightly its LC concentration to satisfy the mass balance. Thermodynamics states that the nematic phase must be at equilibrium with both the α- and β-phases. Therefore, it may be segregated independently from both liquid phases, a fact that may lead to two different average domain sizes (in general a bimodal distribution of nematic domains should be expected when the I−I phase separation precedes the formation of a nematic phase).

Let us consider the system at $T = 28.7$ °C, i.e., in the region where three macroscopic phases coexist at equilibrium. At this temperature the volume fraction and compositions of different phases are α-phase ($1 - R - S = 0.8147$, $\phi_1^{\alpha} = 0.4549$), β-phase ($R = 0.0906$, $\phi_1^{\beta} = 0.7576$), and N-phase ($S = 0.0947$, $\phi_1^{N} = 0.9670$). The fractionation of the thermosetting polymer among the three phases is shown in Figure 8 (calculations were performed with 3360 E_{ij} species). A segregation of residual monomers and low molar mass species to the

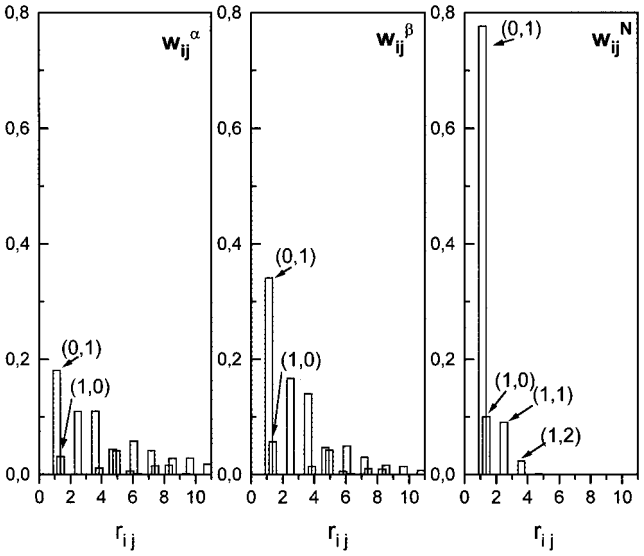

Figure 8. Distribution of the thermosetting polymer in α-, *β*- and nematic phases for the epoxy−E7 blend ($\phi_{LC}° = 0.531$, $T = 28.7$ °C, $p = 0.45$); w_{ij} is the mass fraction of the (*i*,*j*) species where *i* is the number of DA units and *j* is the number of DGEBA units; r_{ij} is the molar volume of the (*i*,*j*) species relative to the molar volume of E7.

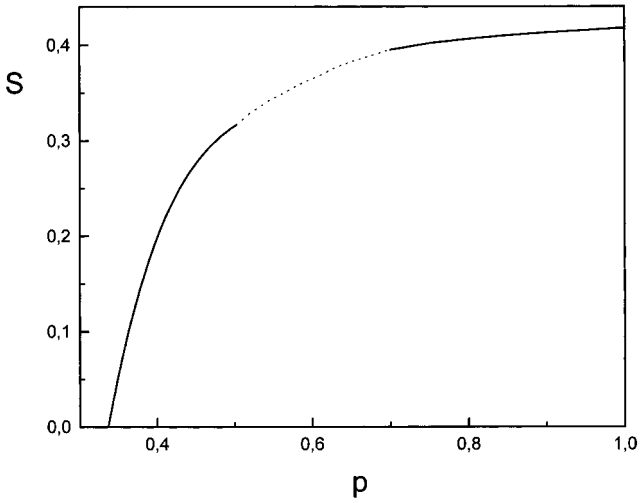

Figure 9. Volume fraction of the nematic phase as a function of conversion for the isothermal polymerization of the epoxy−E7 blend ($\phi_{LC}° = 0.531$), at 20 °C.

nematic phase is clearly observed. This is the result of the exclusion of high molar mass species by the LC. Besides, the *β*-phase is richer in low molar mass species than the α-phase. Number-average degrees of polymerization of the epoxy-amine oligomers in the three phases are: $x_n^{\alpha} = 3.068$, $x_n^{\beta} = 1.991$ and $x_n^{N} = 1.222$. Corresponding polydispersities are $(x_w/x_n)^{\alpha} = 2.779$, $(x_w/x_n)^{\beta} = 1.778$, and $(x_w/x_n)^{N} = 1.100$.

Advancing the conversion at a constant temperature located below the $S = 0$ curve of Figure 5 produces a continuous increase in the volume fraction of nematic phase. Figure 9 shows this trend for a polymerization temperature equal to $T = 20$ °C. Most of the nematic phase is segregated in a relatively short conversion range in the pregel stage. The evolution of the equilibrium composition of both phases is shown in Figure 10. The isotropic phase ends with a LC content equal to $\phi_{LC}^{\alpha} = 0.195$, and the nematic phase consists of pure LC (there is no sol fraction at full conversion).

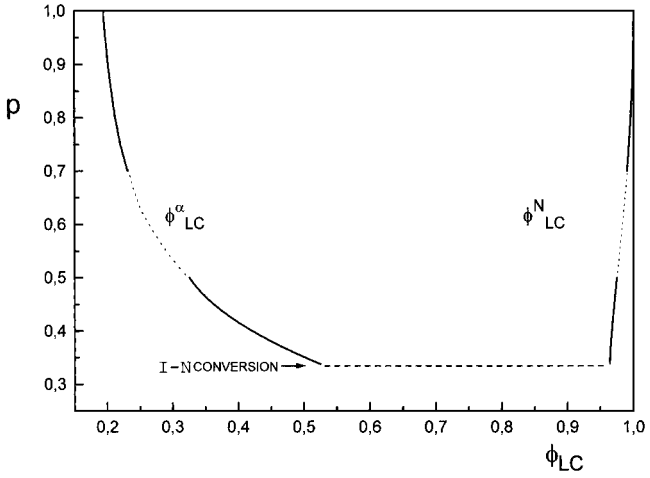

Figure 10. Evolution of the equilibrium composition of phases generated when polymerizing the epoxy−E7 blend ($\phi_{LC}° = 0.531$), at 20 °C to full conversion.

The thermodynamic analysis provides a frame for the evolution of the system in terms of equilibrium compositions and volume fractions of different phases. The actual evolution, i.e., the approach to the equilibrium condition, will depend on the ratio of phase separation rate and cooling or cure rates. Resulting morphologies will strongly vary with the selected trajectory in the temperature vs conversion transformation diagram (Figure 5). It may be predicted that phase separation initiated at low conversions and corresponding low viscosities, should lead to large domains of the nematic phase.[21] This would be the case of an isothermal cure at 20 °C. On the contrary the reaction may be advanced to a high conversion at 100 °C, producing a gel−liquid phase separation in the postgel stage, and then cooled to yield a nematic phase. The nematic domains resulting from this trajectory should be of smaller size. This was indeed the case. For example, the morphology of the epoxy−E7 blend ($\phi_{LC}° = 0.531$), polymerized at 30 °C to full conversion, consisted of a dispersion of spherical domains with an average diameter close to 25 μm. When the same blend was polymerized at 100 °C to a conversion $p = 0.76$, cooled to 30 °C, and reacted at this temperature to full conversion, the nematic domains exhibited an average diameter of about 2 μm.[22] Knowledge of the phase transformation diagram provides a basis for the selection of trajectories leading to different morphologies of the resulting PDLC's (polymer-dispersed liquid crystals).

Conclusions

The consideration of the polydispersity of the polymer in the thermodynamic analysis of polymer−LC blends led to the presence of a temperature region in the phase diagram where three macroscopic phases, two isotropic and one nematic, coexist at equilibrium. The molar mass distribution of the polymer was shown to be significantly different in the three phases. Those richer in LC exhibited an exclusion effect toward the high molar mass fraction of the polymer distribution. This was particularly evident in the nematic phase, which only accepted the low molar mass fraction of the polymer distribution, i.e., monomers and some dimers and trimers in the case of a thermosetting polymer.

In conditions where the appearance of a nematic phase is preceded by a L−L or gel−L phase separation,

the new phase may be segregated simultaneously from both macroscopic coexisting phases. This may lead to a bimodal distribution in the morphologies of nematic domains. Trajectories producing a single isotropic − nematic phase separation process may be selected for the thermoplastic−LC blend and the thermoset−LC blend. In the first case this is accomplished by the use of LC concentrations lower than a limiting value, i.e., $\phi_{LC}° < 0.558$ for the system described in Figure 2. In the latter, single I−N phase separation may be produced by polymerizing at a temperature lower than a limiting value, i.e., $T < 23$ °C for the epoxy-LC blend ($\phi_{LC}° = 0.531$) with a phase transformation diagram shown in Figure 5. Selecting different trajectories in phase diagrams is a way to produce different morphologies starting from the same blend composition. This possibility was proved for the epoxy−E7 blend where the average size of dispersed domains could be changed from 2 to 25 μm by changing the cure cycle.

Acknowledgment. The financial support of the CONICET (Argentina)−CNRS (France) cooperation agreement is gratefully acknowledged.

References and Notes

(1) Kronberg, B.; Patterson, D. *J. Chem. Soc., Faraday Trans.* **1976**, *72*, 1686.
(2) Kronberg, B.; Bassignana, I.; Patterson, D. *J. Phys. Chem.* **1978**, *82*, 1714.
(3) Dubault, A.; Casagrande, C.; Veyssie, M. *Mol. Cryst. Liq. Cryst.* **1982**, *72*, 189.
(4) Ballauff, M. *Mol. Cryst. Liq. Cryst. Lett.* **1986**, *4*, 15.
(5) Ballauff, M. *Mol. Cryst. Liq. Cryst.* **1986**, *136*, 175.
(6) Orendi, H.; Ballauff, M. *Liq. Cryst.* **1989**, *6*, 497.
(7) Kelkar, V. K.; Manohar, C. *Mol. Cryst. Liq. Cryst.* **1986**, *133*, 267.
(8) Shen, Ch.; Kyu, T. *J. Chem. Phys.* **1995**, *102*, 556.
(9) Maier, W.; Saupe, A. *Z. Naturforsch., A* **1959**, *14*, 882.
(10) Maier, W.; Saupe, A. *Z. Naturforsch., A* **1960**, *15*, 287.
(11) Borrajo, J.; Riccardi, C. C.; Williams, R. J. J.; Masood Siddiqi, H.; Dumon, M.; Pascault, J. P. *Polymer* **1998**, *39*, 845.
(12) Ahn, W.; Kim, C. Y.; Kim, H.; Kim, S. C. *Macromolecules* **1992**, *25*, 5002.
(13) Peebles, L. H. *Molecular Weight Distributions in Polymers*; Interscience: Wiley: New York, 1971.
(14) Stockmayer, W. H. *J. Polym. Sci.* **1952**, *9*, 69.
(15) Stockmayer, W. H. *J. Polym. Sci.* **1953**, *11*, 424.
(16) Masood Siddiqi, H.; Dumon, M.; Eloundou, J. P.; Pascault, J. P. *Polymer*, in press.
(17) Borrajo, J.; Riccardi, C. C.; Williams, R. J. J.; Cao, Z. Q.; Pascault, J. P. *Polymer* **1995**, *36*, 3541.
(18) Riccardi, C. C.; Borrajo, J.; Williams, R. J. J.; Girard-Reydet, E.; Sautereau, H.; Pascault, J. P. *J. Polym. Sci. B: Polym. Phys.* **1996**, *34*, 349.
(19) Miller, D. R.; Macosko, C. W. *Macromolecules* **1976**, *9*, 206.
(20) Miller, D. R.; Valles, E. M.; Macosko, C. W. *Polym. Eng. Sci.* **1979**, *19*, 272.
(21) Williams, R. J. J.; Rozenberg, B. A.; Pascault, J. P. *Adv. Polym. Sci.* **1997**, *128*, 95.
(22) Masood Siddiqi, H.; Dumon, M.; Pascault, J. P. *Mol. Cryst. Liq. Cryst.*, in press.

MA971206W